Robust Computer-Assisted Laser Treatment Using Real-time Retinal Tracking

Nahed H. Solouma, Abou-Bakr M. Youssef, Yehia A. Badr, and Yasser M. Kadah
Biomedical Engineering Department and Laser Institute, Cairo University, Giza, Egypt, Email: ymk@internetegypt.com

Abstract- **We propose a new computerized system to accurately guide laser shots to the diseased areas within the retina based on predetermined treatment planning. The proposed system consists of a fundus camera interfaced to a computer that allows real-time capturing and processing of a sequence of images at video frame rates. The first image in the sequence is used as a reference for manual treatment planning. A new segmentation technique was developed to discern the blood vessel tree in which we extract the boundaries of the wide vessels as well as the whole lumen of smaller ones. The core of wide vessels is then obtained by correlating the image with a 1-D Gaussian filter in two perpendicular directions and thresholding the result. A fast registration technique is proposed to automatically track the motion of segmented areas within the subsequent images in the sequence. In this technique, points satisfying certain developed significance conditions are chosen as landmarks in the reference frame. Using the extracted set of corresponding points in the subsequent image frames, we can accurately align image frames to compensate for eye movements and saccades. The new technique has the potential to significantly improve the success rates in this type of treatment.**

Keywords-**retinal tracking, contour detection, feature extraction, image registration**

I. Introduction

Diabetic retinopathy resulting from long term diabetes mellitus is one of the common diseases that lead to choroidal neovascularization (CNV). CNV is considered among the leading causes of blindness [1]. Among the currently available treatment methods, laser can be used to photocoagulate the diseased areas. To obtain satisfactory results, the physician must identify the full extent of CNV and cauterize it completely in order to save the central vision [1-2]. Several thousand laser shots are usually required during such treatment. Moreover, special care must be taken to avoid hitting the blood vessel tree, the macula, the optic disk, and the region between them. For a single eye, this procedure requires up to several hours that are usually divided over many treatment sessions [1-2].

Even though laser treatment has been shown to be superior to the other available methods, it suffers from a number of serious problems. The current success rate of this procedure is below 50% for eradication of CNV following one treatment session with a recurrence and/or persistence rate of about 50% [2]. The latter condition requires repeating the treatment and each treatment repetition in turn has a 50% failure rate. Several studies have indicated that incomplete treatment was associated with poorer prognosis than no treatment at all [2]. Consequently, the development of an accurate laser treatment guidance system to treat the whole retina in one session would have a strong impact on the effectiveness of such procedures.

In this work, we propose a new computerized treatment planning system for laser treatment of CNV. The new system has the potential to improve the accuracy of the procedure thus lowering its failure rate while maintaining the same treatment time. A major part of this system is the tracking the retina using a computer-controlled system that captures and processes retinal images from a fundus camera. Novel image processing routines are applied to the retinal images to determine the correct positions for laser shots on the retina. In particular, an accurate segmentation procedure is applied to the first retinal image to extract the sensitive areas in the retina. Subsequently, this segmentation is continuously updated using a fast registration procedure to obtain the new positions in case of eye movement at real-time rates. These positions can be fed to a beam steering apparatus that precisely directs the laser beam accordingly. The new system is demonstrated on real data and its performance is analyzed.

II. Data Acquisition

A block diagram of the data acquisition system is presented in Fig. 1. The retinal images are acquired using a TOPCON TRC-501A fundus camera. A Sony Charge Coupled Device (CCD) video camera is attached to the eyepiece of the fundus camera to make its images available in standard video format. The video output from the CCD camera is interfaced to a Micron PC (700 MHz processor, 128Mbytes of RAM) through a Matrox Meteor video digitizer card. The retinal images are captured into the memory of the computer either as individual frames or as a real-time video sequence. The size of each frame is 640x480 pixels of gray-level images.

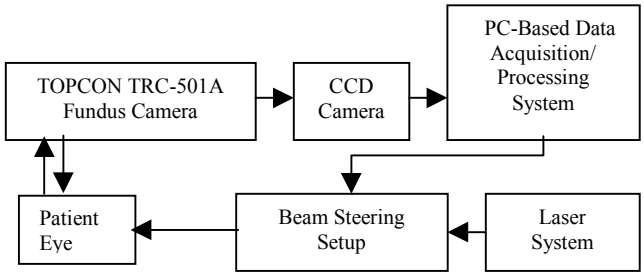

Figure 1: a block diagram for retinal tracking system.

III. Methods

A. Contour Detection

Contour detection is performed using deformable models. This technique is an iterative process in which we initialize an active contour model close to the contour of interest. This contour deforms in such a way that it converges to the true

Report Documentation Page

Report Date	Report Type	Dates Covered (from... to)
25 Oct 2001	N/A	-

Title and Subtitle Robust Computer-Assisted Laser Treatment Using Real-Time Retinal Tracking	**Contract Number**
	Grant Number
	Program Element Number
Author(s)	**Project Number**
	Task Number
	Work Unit Number
Performing Organization Name(s) and Address(es) Biomedical Engineering Department and Laser Institute Cairo University Giza, Egypt	**Performing Organization Report Number**
Sponsoring/Monitoring Agency Name(s) and Address(es) US Army Research, Development & Standardization Group (UK) PSC 802 Box 15 FPO AE 09499-1500	**Sponsor/Monitor's Acronym(s)**
	Sponsor/Monitor's Report Number(s)

Distribution/Availability Statement
Approved for public release, distribution unlimited

Supplementary Notes
Papers from 23rd Annual International Conference of the IEEE Engineering in Medicine and Biology Society, October 25-28, 2001, held in Istanbul, Turkey. See also ADM001351 for entire conference on cd-rom.

Abstract

Subject Terms

Report Classification unclassified	**Classification of this page** unclassified
Classification of Abstract unclassified	**Limitation of Abstract** UU

Number of Pages
4

vessel contour. This is achieved using an iteration that minimizes energy functional of the form:

$$\varepsilon = \Sigma\ (\varepsilon_{internal}\ (v(s)) + \ \varepsilon_{external}(v(s))), \qquad (1)$$

where v(s**)** is a parameterized contour that is normally represented by a discrete set of points or *snaxels* $\{v_1,..,v_n\}$, $\varepsilon_{internal}(v(s))$ is the internal energy of the contour due to the elastic deformation and bending of the contour, and $\varepsilon_{external}(v(s))$ represents the energy due to image forces such as lines, edges, termination of line segments and corners [4]. The steady-state position of the contour is the one it takes when its energy is at minimum. The contour model is deformed using one of many algorithms for searching the neighboring points of each snaxel to extract the point of minimum energy, which will then become the new snaxel [4].

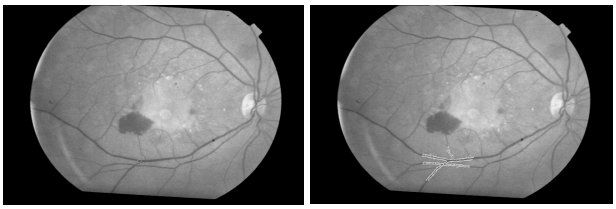

Figure 2: Initial contour (left) and after 50 iterations (right).

In applying deformable models to retinal images to detect the boundaries of the blood vessel tree, the initial contour has to grow and converge to the edges of the vessel. The contour growth could be achieved by interpolating the points on the contour. Also, in order to obtain useful results, many constraints and user interaction were needed which limit the practicality of the procedure. Here, we tried to minimize the number of required computations and make the process as close to being automatic as possible at the highest attainable accuracy. In particular, we studied the effect of the internal energies and compared it with the effect of the external energy (edge energy in this case) to make sure that the effect of the external energy will be dominant. The image was convolved by a Sobel operator in both the horizontal and vertical directions [4]. The magnitude of the result was used to represent the external energy of the contour. Instead of selecting a single point having the minimum energy (i.e., maximum edge value) from the neighborhood of each snaxel, we search all the neighboring points of each snaxel and extract all the points having a value above certain threshold as new points on the contour. This not only deforms the contour but also makes it grow.

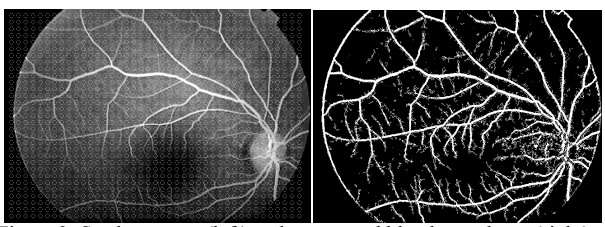

Figure 3: Seed contours (left) and segmented blood vessel tree (right).

B. Detection of the blood vessel tree

Instead of manual initialization of contours, the whole image was covered automatically with an initial set of small contours called *seed* contours (see left image in Fig. 2) [5]. During the contour iteration convergence and growth, the seed contours that lie within the areas of poor edges shrink until vanishing. The others will merge and/or split until recovering a continuous description of all edges that pass above a certain threshold. This threshold changes for each iteration to allow for faster and more accurate convergence. This process is repeated until no changes occur during a given iteration. This process leads to the complete detection of all small vessels in addition to the boundaries of the larger ones. The intensity values across blood vessels are usually assumed to have a Gaussian distribution. On the other hand, the small segments usually have repeated intensity values. So, correlating the image with two-dimensional filters of suitable size (e.g., 16x15) can provides reasonable results but requires a large number of computations to detect all vessels. In particular, the filter has to be applied in 12 different directions to detect vessels in all possible directions. Since we detect the small vessels and the boundaries of the wider vessels at an earlier step, we only need to obtain the core of the wide vessels. Therefore, we only have to correlate the image with two one-dimensional Gaussian filter

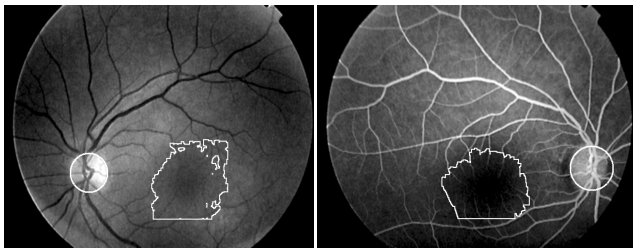

Figure 4: Examples of demarcation of the optic disc and the macula.

in the vertical and the horizontal directions only. This reduces the computational complexity of the original technique to a great extent and makes it practical for clinical applications. Fig. 2 shows the seed contours and the result of applying this technique.

C. Segmenting the optic disc and the macula

The optic disc is a well-delineated object with properly defined size and edges. In the gray level retinal images, it always appears as nearly circular structure that is brighter than the background of the retina. So, the Hough transform [7], which is well known robust method to extract circular objects, was used to detect the center and the radius of the optic disc. A circle was drawn around the optic disc and this circle was filled to distinguish this structure.

The macula is the area of acute vision within the retina. It appears as the most homogeneous area near the optic disc. To segment the macula, we used a region-growing algorithm to demarcate the macula [7]. Fig. 3 shows the result of applying these techniques on retinal images with Indocyanine Green

contrast (which appears as bright blood vessels in a dark background) as well as normal images.

D. Estimating the locations of laser shots

After extracting all sensitive objects that must be avoided during laser treatment, a binary image was composed containing these objects. This image was dilated by a square structuring element of dimensions 7x7 to maintain a safety margin around these sensitive areas. The locations of shots were determined and spaced in the background (see Fig. 4). These locations are stored in the database of the patient and get updated with every successive image frame [7].

E. Real-time movement tracking

Since the segmentation step is rather time consuming, it is not possible to use it to track fast eye movements particularly during the laser treatment session. Alternatively, we only use segmentation for the first (reference) retinal image and then the segmentation of any subsequent frame is obtained through fast registration with this reference. Since the retinal motion is expected to follow a rigid body motion model (except in case of retinal tears), we developed an algorithm to extract some points (landmarks) and get their relation relative to certain point. Then we find their corresponding points in the subsequent frames.

Algorithm for detection of candidate landmarks

1. Start with a reference image R , a current image C, a threshold t and a one-dimensional filter f defined as [4,3,2,1,–2,–5,–6,–5,–2,1,2,3,4].
2. Estimate *RefC*, the optic disc center, using Hough transform.
3. Correlate R with f and threshold above t. let the result be called *RR*.
4. Perform morphological thinning of *RR* by one pixel.
5. Let *temp* = sum of a 5x5 window over every pixel in *RR*.
6. Let *RefLandmarks* be the points in *temp* that are greater than 5 (points of branching and cross over). We get n points.
7. If there are some connected points, take only the central point. Hence, the number of points reduces to m points.
8. Take a window around the optic disc center and get the corresponding image called *CurrentC* in the subsequent frames by template matching.
9. Repeat steps 3-7 for the current image C to obtain the *CurrentLandmarks* as m points.

Then, we have a set of reference landmarks and a set of current landmarks.

Algorithm to obtain the corresponding pairs

1. Take *RefC* as the point of origin and compose m vectors for the m points in *CurrentLandmarks*.
2. Compute the slope of every pair.
3. Repeat steps 1-2 for *CurrentC* to obtain n vectors. Every pair in the reference set may have a corresponding pair in the current set.
4. Calculate the angle of rotation for every two pairs.
5. Extract the pairs of angles with absolute angle magnitudes between 4 and 6 or less than 1.
6. Transform each of the points in *RefLandmarks* by an affine transformation matrix corresponding to the extracted rotation angle.
7. Find points in *CurrentLandmarks* that are close to the result of transformation. Then we have a set of reference points and their corresponding points in the current image.
8. Take the mean angle of rotation and the mean shifts to be the motion parameters.
9. Transform the position of laser shots in the reference frame to their corresponding positions in the current frame using the computed motion model.

It should be noted here that one could use the vector length instead of the transformation matrix for a faster response at still reasonable results.

IV. Results and Discussion

The results of segmenting the blood vessel tree are shown in Fig. 3. As can be observed, the proposed algorithm gives accurate results. The grid of seed contours makes the process close to being automatic. Fig. 4 shows an example of demarcation of the optic disc and the macula. After extracting all of the sensitive areas in the reference frame, we locate the laser shots away from these objects. The center of the optic disc was shown to be an excellent landmark between different image in the acquired image sequence. This is mainly because the gray scale pattern around this center cannot be matched anywhere else within the image. This is important to make the registration process more robust.

The method suggested for landmark estimations used the same criteria in all image frames. So, we expect it to give fairly accurate list of candidate landmarks for subsequent matching in our registration procedure. Fig. 5 shows an example of the obtained landmarks in the reference and another image in the sequence of images following the reference image. As can be seen, most of these landmarks have correct match in the other image, which indicates the success of the proposed matching procedure. Fig. 6 shows two example of mapping the laser shots in normal images (top pair) as well as Indocyanine Green images (bottom pair). The results show an accurate mapping of laser shot locations between the reference (left) images and the other image on the right. This demonstrates the success of the proposed technique in tracking the motion of the retina and correcting the target laser shot locations accordingly.

It is important to comment on the computational complexity of the proposed algorithm. The first part of the technique involving the segmentation of the blood vessel tree from the reference image has the highest computational complexity in the new method. The exact time required for doing this task varies from image to another. Nevertheless, the observed typical time required for such procedure was between 4-7 sec on the data acquisition computer system described above. This time is not crucial for our real-time processing goal since this processing is done prior to the actual laser treatment. Therefore, the time to extract and match the landmarks to register other

images to that reference image is the most important for the practicality of the proposed method. The computations of this part may also vary between different images in the sequence. The computational times we measured for our experiments provided results in the range between 0.2 and 0.3 sec, which is considered practical for on-line use. Using a more powerful computing platform (which is now widely available commercially) can bring this time lower.

Even though the proposed technique shows a large potential for clinical application, several limitations are yet to be addressed for more robust performance. Some pathological cases involve dramatically different retinal image morphology that would break the assumptions used in this work. An example of this is the case where noncircular optic disk. Moreover, the proposed technique cannot handle large scale, contrast or illumination changes among images within the acquired image sequence. Such changes may result from normal effects like fading contrast agent or gross motion. It is therefore recommended that the reference image be updated periodically during the laser treatment session. This helps keep the acquired images always within an acceptable range from the reference image. Another limitation in computing the rotational motion component is the limited resolution of images. This result in approximating fractional laser shot locations into their nearest integer coordinates. As a result, the accuracy of the derived laser shot locations cannot get any better than half a pixel.

V. Conclusions

A new computerized technique for laser treatment planning was proposed. The new technique performs accurate segmentation on a reference frame. The locations of the laser shot on this reference image are then recomputed for the sequence of images acquired during the treatment using fast registration. This enables fast tracking of retinal structures and ensures proper administration of the treatment in case of eye movement. The proposed technique was applied to real data and the results showed a large potential for its clinical application.

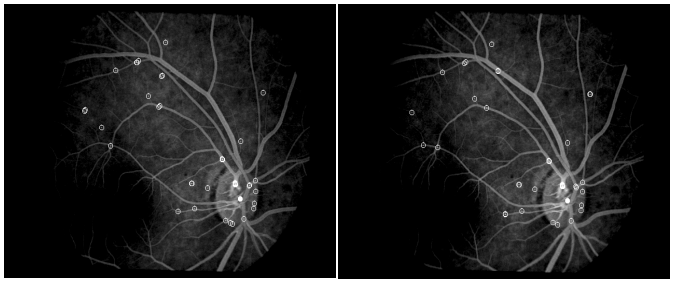

Figure 5: Landmarks in reference image (left) and a subsequent image (right).

Acknowledgment

This work was supported in part by IBE Technologies, Egypt.

References

[1] S.L. Trokel, "Lasers in ophthalmology," *Optics,Photonics News*, pp. 11-13, Oct. 1992.

[2] D.E. Becker, A. Can, J.N. Turner, H.L. Tannenbaum and B. Roysam, "Image processing algorithms for retinal montage synthesis, mapping, and real-time location determination," *IEEE Trans. Biomed. Eng.*, vol. 45, no. 1, pp. 105-117,1998.

[3] R.M. Haralick, S.R. Sternberg and X. Zhuang, "Image analysis using mathematical morphology," *IEEE Trans. Pat. Anal. Mach. Intell.*, vol. 9, no. 4, pp.532-550, 1987.

[4] T. McInerney and D. Terzopoulos, "Topologically adaptable snakes," *Proc. Int. Conf. Computer Vision (ICCV)*, pp. 840-843, June 1995.

[5] S. Chaudhuri, C. Chatterjee, N. Katz, M. Nelson, and M. Goldbaum, "Detection of blood vessels in retinal images using two-dimensional matched filters," *IEEE Trans. Med. Imag.*, vol. 8, no. 3, pp.263-269, 1989.

[6] D.I. Barnea and H.F. Silverman, "A class of algorithms for fast digital image registration," *IEEE Trans. Comp.*, vol. 21, no.2, pp.179-186, 1972.

[7] B. Peli, R.A. Augliere and G.T. Timberlake, "Feature-based registration for retinal images," *IEEE Trans. Med. Imag.*, vol. 6, no. 3, pp.272-278, 1987.

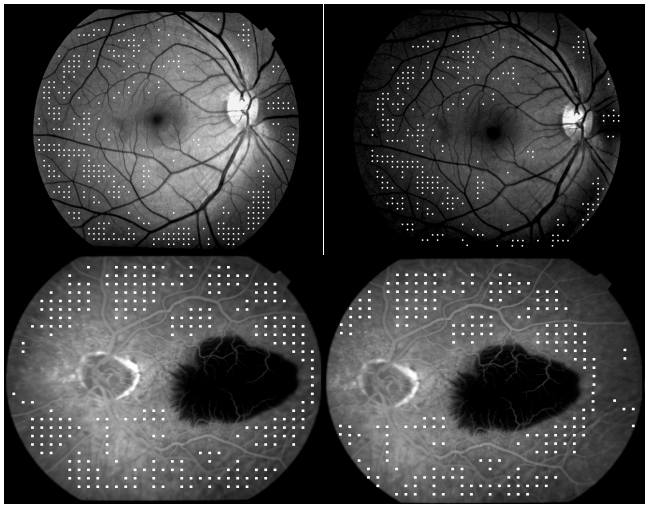

Figure 6: The reference location of laser shots (left images) and the transformed location (right images).